AIAA JOURNAL
Vol. 30, No. 6, June 1992

Strength of Laminated Composites with Internal Discontinuities Parallel to the Applied Load

Anthony J. Vizzini*
University of Maryland, College Park, Maryland 20742

A methodology to predict the strength of laminated composites with internal discontinuities parallel to an uniaxially applied load is developed. A quasi-three-dimensional finite element analysis is used to determine the state of stress at and near the internal discontinuity. Two techniques to predict the strength are developed. In one technique, the state of stress in a small resin pocket at the discontinuity is used with an isotropic failure criterion to determine the strength of the discontinuity. The other technique uses the in-plane state of stress around the discontinuity with a failure criterion based on an analogy with an individual ply. A limited number of specimens that had either a longitudinal ply drop or a material discontinuity were manufactured and tested in uniaxial tension. Damage initiation was detected via a load drop that corresponds to an increase in the compliance of the specimen. The observed response of the specimens agrees well with the predictions.

Introduction

An initial advantage of using composite materials in aerospace applications is their relatively high specific strength and stiffness. However, design considerations go beyond a simple decrease in weight for a given strength or stiffness requirement. Composites are sought for applications where the designer can tailor the component by specifying the local elastic properties rather than be constricted by isotropic constraints of metals or even the constraint of a single layup throughout the component. It is possible to generate designs where each ply in the component is described by its material and orientation. Moreover, restrictions on any given ply are removed via techniques such as ply termination and fiber placement. Thus, a component is not restricted to have the same makeup through the thickness.

Significant work has been done on lengthwise tapered specimens that vary the thickness of the component along the primary loading direction. [1-3] In these lengthwise tapered sections the material discontinuity is perpendicular to the applied load, as shown in Fig. 1. The stress state in the taper region is three-dimensional. The interlaminar stresses that arise often control the strength of the component by leading to delamination in the taper region. However, not all applied loads will be perpendicular to the taper and, in general, will be at an arbitrary orientation. In particular, a widthwise taper results in a component with a constant cross section along the length, but of varying thickness across the width, as shown in Fig. 1. If an isotropic material were to be used, the stress would be uniform throughout the cross section and in the plane of the applied loading. However, such a disturbance in the cross section of a laminated composite component will cause a three-dimensional state of stress.[4]

A discontinuity perpendicular to the orientation of the applied load causes a significant redistribution of stresses as the load path must adjust itself around the discontinuity. Similarly, an internal discontinuity such as a longitudinal ply drop or a material discontinuity can be the limiting factor in the overall strength and performance of the component. Discontinuities parallel to the applied load represent a simple case that must be understood in order to predict the strength and response of tailored composite structures.

In a previous experimental study,[5] laminates with internal discontinuities parallel to the load direction were loaded under uniaxial tension. These laminates either had a ply drop or a material discontinuity that ran the entire length of the specimen. Post mortem analysis of the failed specimens often indicated that damage initiated at the internal discontinuity. The objective of this study is to provide a methodology to predict the onset of damage at such an internal discontinuity and, thus, the failure of the internal discontinuity. Delamination failure of the ply interfaces at the internal discontinuity is not considered.

Finite Element Stress Analysis

Description

The two types of internal discontinuities considered in this study involve a longitudinal ply drop or a discontinuous reorientation of a ply as shown in Figs. 2 and 3. Here the stress-free edge is removed far enough from the internal discontinuity so that the interlaminar stress state at the free edge does not influence the stress state at the internal edge.

To designate either internal discontinuity, a vertical line is used in the laminate notation. Thus, the notation $\theta|\alpha$ designates that the θ ply is originated at the center of the specimen, is terminated at the internal edge, and then is continued with the same material at an orientation of α. A longitudinal ply drop is designated as $\theta|$ because no ply is continued past the internal edge.

The response of the component with an internal discontinuity can be assessed in terms of the stress distribution at the internal edge. The state of stress at the internal discontinuity is determined using a quasi-three-dimensional finite element approach with a 12 degree-of-freedom assumed-stress hybrid element based on the Hellinger-Reissner principle.[6,7] In all cases, a six-ply, symmetric laminate with internal discontinuities symmetric about the centerline and the midplane are considered. Only one-quarter of a typical cross section is modeled due to the symmetry considerations. A total of 20 elements are used in the width direction and 10 elements in the thickness direction. The finite element meshes in the vicinity of the discontinuities are shown in Figs. 2 and 3. The modeled cross section is placed under an uniform uniaxial strain and the deflections u, v, and w at each node are determined. The state of stress, averaged for each element, is then determined.

Presented as Paper 90-1065 at the AIAA/ASME/ASCE/AHS/ASC 31st Structures, Structural Dynamics, and Materials Conference, Long Beach, CA, April 2-4, 1990; received May 30, 1991; revision received Sept. 30, 1991; accepted for publication Oct. 1, 1991.

*Assistant Professor, Composites Research Laboratory, Department of Aerospace Engineering. Member AIAA.

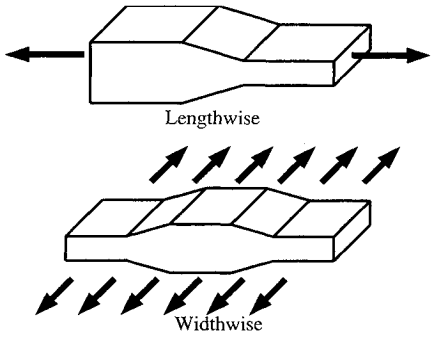

Fig. 1 Lengthwise and widthwise tapers.

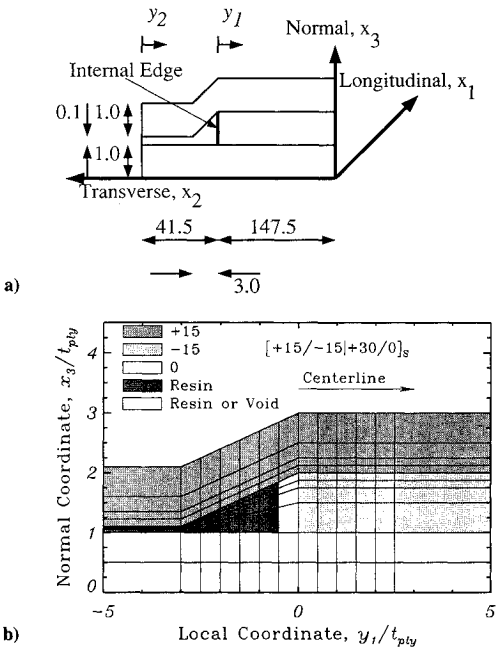

Fig. 2 Longitudinal ply drop: a) normalized dimensions; b) finite element grid.

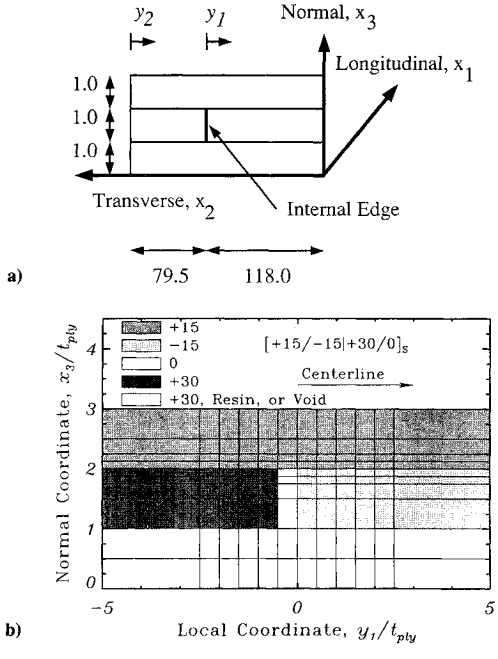

Fig. 3 Material discontinuity: a) normalized dimensions; b) finite element grid.

Table 1 Material properties

AS4/3501-6			
Elastic constants		In-plane strength	
E_L	147.2 GPa	X^t	2300 MPa
$E_T = E_N$	9.65 GPa	X^c	1400 MPa
$\nu_{LT} = \nu_{LN}$	0.3	Y^t	54 MPa
ν_{TN}	0.54	Y^c	221 MPa
$G_{LT} = G_{LN}$	6.84 GPa	S^{LT}	105 MPa
G_{TN}	5.5 GPa		
t_{ply}	0.134 mm		

3501-6 Neat Resin			
Elastic constants		Strength	
E	3.5 GPa	σ_0	54 MPa
ν	0.3		

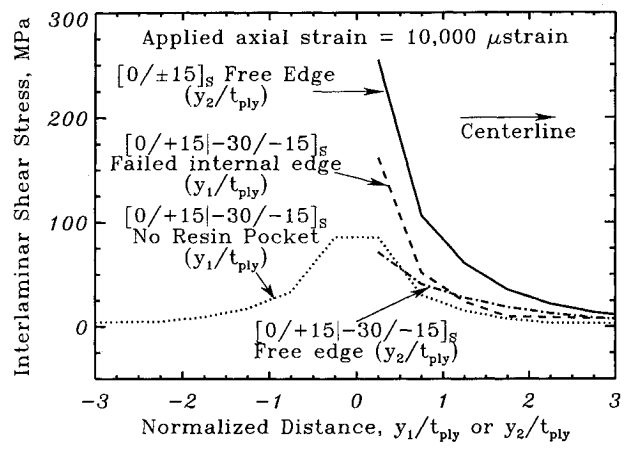

Fig. 4 Interlaminar shear stresses at free and internal edges.

The internal discontinuity between two plies is modeled in one of three ways: no resin pocket, resin pocket, and failed. The only difference between the three models is what is assumed for the elements adjacent to the discontinuity. In the model without a resin pocket, the elements to the left of the discontinuity (the white elements in Fig. 3) are the same material and orientation of the terminated ply to the left of the discontinuity. In the model with a resin pocket, these elements are set to the matrix material, and the stresses in the resin pocket are determined. Finally, in the model with a failed interface, the stiffness of these elements is set to zero, and the stresses around the failed interface are determined.

The physical dimensions normalized by the nominal ply thickness used in the models are shown in Figs. 2 and 3. In addition, two local coordinates are defined in the figures. The local coordinate y_1 is measured from the internal edge, and the local coordinate y_2 is measured from the free edge. Both local coordinates are measured positive toward the centerline of the specimen.

The stress state is determined for a longitudinal strain of 10,000 microstrain applied uniformly over the entire cross section. The stress is any one element is the average of the stress values at four Gaussian integration points within the element. The material used throughout the analysis is AS4/3501-6 graphite/epoxy. The material properties for AS4/3501-6 and the net resin are provided in Table 1.

Internal Edge

The strength of the internal discontinuity can be determined from the state of stress at and near the discontinuity. Figure 4 shows typical interlaminar shear stresses at the $+15/-15$ interface in a $[0/+15|-30/-15]_s$ laminate. For comparison, the interlaminar stress at the free edge of a $[0/\pm15]_s$ laminate is also given. The finite element model indicates a significant

reduction of the interlaminar shear stress at the free edge, the dominant contributor to failure of the $+15/-15$ interface in a $[0/\pm 15]_s$. Moreover, the interlaminar shear at the internal edge is also not significant when the +15-deg ply is terminated and continued with a −30-deg ply. Delamination failure of the $+15/-15$ interface at the internal discontinuity is likely to occur at strain levels appreciably higher than the level at which the same interface would delaminate at the free edge. Thus, the failure of the internal edge will occur prior to any delamination at the internal edge.

In-plane

For the cases with a material discontinuity, the in-plane stress is evaluated at the center of the elements along either side of the discontinuity. To approximate the stress state at the discontinuity, the state of stress of the elements on both sides of the discontinuity are averaged.

The strength of an internal discontinuity involving a discontinuous angle alteration is not apparent from the calculated stress state in the laminate coordinate. Clearly, if the transverse stress σ_{22} is greater than the transverse tensile ultimate of the basic unidirectional ply, failure will occur. Thus, the discontinuity is idealized, as in Fig. 5. For strength considerations only, the gap between the two angled plies is considered as the gap between parallel fibers in an unidirectional ply. In this way, the strength of the internal discontinuity is characterized by the strength of a unidirectional ply oriented in the same direction as the discontinuity. Thus, the in-plane stress state is resolved in the axes of the discontinuity. This method is not valid whenever the local stress state would cause failure of either of the adjacent materials.

Resin Pocket

Realistic manufacturing techniques of a material discontinuity involving plies butted together will result in a resin-rich zone between the two plies. Resin-rich layers are known to exist between laminae through the thickness and are assumed to exist at material discontinuities in this study.

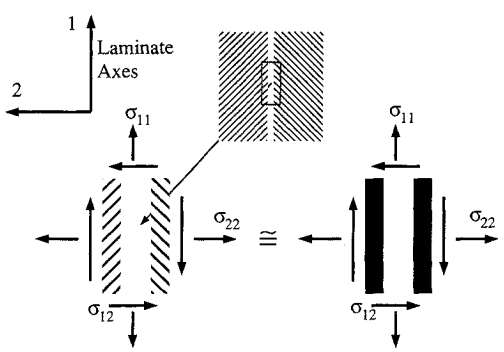

Fig. 5 Comparison of material discontinuity with unidirectional ply.

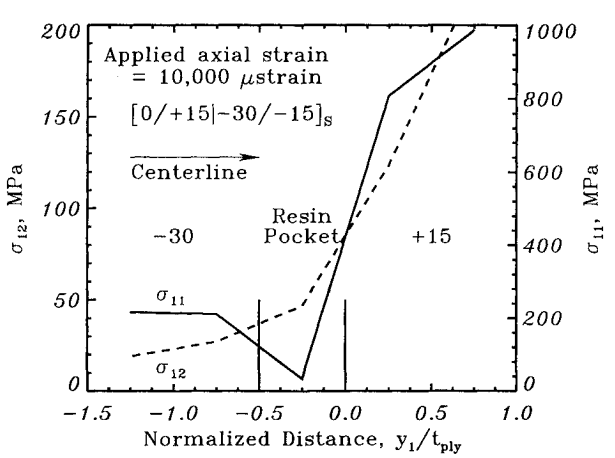

Fig. 6 In-plane stresses within the resin pocket.

In the finite element model shown in Fig. 3, the elements on the left side of the discontinuity represent this resin-rich pocket. Now the state of stress is evaluated within the resin pocket directly. Typical results are shown in Fig. 6 for the longitudinal stress σ_{11}, and the in-plane shear stress σ_{12}.

Given the stress state in the resin, an isotropic failure criterion can be applied to predict failure. Failure of the internal edge occurs whenever any resin element reaches a critical state of stress. Fracture of the resin pocket will result in an in-plane failure of the internal discontinuity.

The strengths of the specimens with vertical ply drops are determined in a similar manner. In order to use the same basic finite element model throughout the study, the vertical ply drop is modeled by terminating the ply and continuing with a resin region. This resin region tapers from the thickness of one ply at the ply termination to the thickness of the interply matrix layer in three ply thicknesses. Because the stresses are calculated for each element in the model, the state of stress within the resin pocket is known and can be used in the same isotropic failure criterion. Again, fracture of any resin element will result in the failure of the internal discontinuity.

Postfailure

Finally, to determine the effect of an internal discontinuity that has failed, the original finite element model is once again modified by removing the elements at the internal discontinuity. The ply interfaces at the internal discontinuity are now more prone to delamination after failure of the internal discontinuity because the interlaminar stress state increases. This is shown for the interlaminar shear stress in Fig. 4 when the curves titled "$[0/+15|-30/-15]_s$ No resin pocket" and "$[0/+15|-30/-15]_s$ Failed internal edge" are compared. A delamination criterion, such as Ref. 8, may be used to determine whether a delamination occurs at the ply interfaces at the failed internal discontinuity.

Experimental Program

Description

A total of 50 six-ply, tensile coupons were manufactured and tested at the Composites Research Laboratory at the University of Maryland. The specimens had layups of either $[0/\pm 15]_s$ or $[\pm 15/0]_s$. These layups delaminate at the stress-free edge at the $+15/-15$ interface. Five specimens of each layup were tested to generate baseline data. Longitudinal discontinuities were introduced in both layups on either the second and fifth plies or the third and fourth plies. Five specimens were manufactured for each layup, discontinuity, and ply location.

The material used throughout this program was AS4/3501-6 graphite/epoxy manufactured by Hercules. The material is supplied as a preimpregnated 305-mm-wide tape and is cut into 350-mm by 300-mm plies and laid up on a flat aluminum cure plate. All of the discontinuities were introduced into the specimens by removing material of the designated plies during the layup of the laminate. The material was removed by using an aluminum template. The same template was used to cut the material that replaced the removed material. For the longitudinal ply drop, no additional material was added. The angle reorientations in the material discontinuity were originally chosen so as to evenly distribute the interlaminar shear stress over the internal and free edges. The laminate notations of the four layups with material discontinuities are: $[0/+15|-30/-15]_s$, $[0/+15/-15|+45]_s$, $[+15/-15|+30/0]_s$, and $[+15/-15/0|+15]_s$.

All discontinuities were introduced symmetrically about the midplane and centerline of the laminate. The resulting specimen had an unaltered middle section of 38.1 mm in width and two altered edge zones with nominal widths of 5.95 mm each as shown in Fig. 7.

After the discontinuities were introduced and the lay up process was completed, the laminates were cured. Aluminum

and cork dams were used to keep the laminates in place during the cure cycles. The cure took place in an autoclave and followed the manufacturer's recommended cycle of 1 h at 116 °C and 2 h at 177 °C with 590 KPa and a full vacuum (762 mm Hg) applied throughout. All specimens were postcured in the autoclave at 177 °C for eight hours. The specimens were machined to the desired lengths on a milling machine adapted for composites with a water-cooled diamond-grit cutting wheel. Because the location of the internal discontinuity could easily be seen in the cured laminates, the laminates were aligned visually with respect to the blade. Glass tabs were bonded to the specimens with FM-123-2 film adhesive. The bond cure was done at 70 KPa and full vacuum at 107 °C for 2 h.

The thickness of the middle and edge sections and the width of each specimen were measured at several locations in the test section. The average thickness of the unaltered laminates and the unaltered midsection of the altered laminates is 0.80 mm with a coefficient of variation (CV) of 3.3%. The average thickness of the edge zone for the longitudinal ply drop is 0.69 mm (2.2% CV) and for the material discontinuity is 0.80 mm (2.0% CV). The average width of all the specimens is 49.77 mm (0.4% CV).

The specimens were then instrumented with Micro Measurement strain gages (EA06-125AD-120) and (EA06-031DE-120). Each of the unaltered specimens were gaged with a longitudinal and a transverse gage at the center location of the test section. Longitudinal gages were placed in the center of the unaltered section, the center of the edge zone, and over the internal edge for all of the parallel discontinuity specimens. In all cases, the free edges were coated with a white opaquing fluid to increase the visibility of any free-edge delaminations.

All of the specimens were tested on an MTS 810 uniaxial testing machine with hydraulic grips. The specimens were loaded monotonically in tension at a constant stroke rate of 0.762 mm/min, which is equivalent to a strain rate of approximately 3800 microstrain/min for a 200-mm test section.

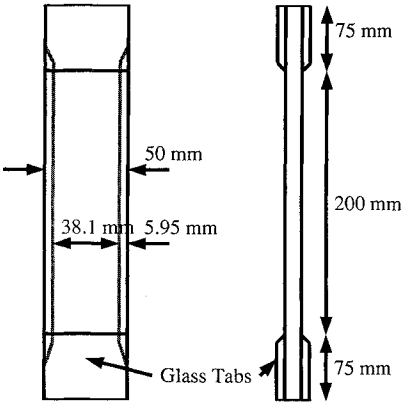

Fig. 7 Parallel discontinuity specimen.

Strain gage and load data were taken automatically at 0.25-s intervals with the use of a computer. The stroke ramp was halted at the first indication of delamination; that is, a drop in load or an audible indication. The free edge was visually inspected, any damage was noted, and the stroke ramp was resumed. This process was repeated until any free-edge delamination was noted. The specimen was then loaded to failure. The failed specimens were photographed, removed from the hydraulic grips, and examined.

Damage Initiation

The exact onset of delamination or damage cannot be determined directly from the data. However, because any damage results in a more compliant structure, a decrease in the applied load for a given longitudinal displacement would indicate that a significant damage event had occurred. A decrease of approximately 90 N between successive load readings was judged to indicate the onset of damage. Any disturbance in the load less than this level was considered to be noise. In most cases, the initial damage point coincided with an audible pop.

Because the thickness of the specimens with a longitudinal ply drop is not constant, there are multiple ways to report the stress at which damage occurred: total load divided by measured area, total load divided by nominal area, or total load divided by the baseline area. Thus, only the laminate strain at the damage event is reported. The value of strain at the center longitudinal gage is used. Because all of the specimens have effectively the same modulus within the unaltered midsection, the longitudinal strain is an indication of the stress of the primary structure. The damage onset strains of all the specimens are given in Table 2.

Failure Sequence

Unaltered $[\pm 15/0]_s$ laminates fail as a result of massive delamination initiating at the free edge between the $+15/-15$ interface that is driven by interlaminar shear stresses.[8] Here delamination initiated at the free edges and occurred across the entire laminate width. This damage is typical of delamination initiated failure. Unaltered $[0/\pm 15]_s$ laminates delaminated at the $+15/-15$ interface at a higher stress level.

When there is discontinuous inteface; that is, a longitudinal ply drop or a material discontinuity, the internal edge plays a major role in the ultimate failure of the laminate. Often, the free edge did not delaminate, but rather a sequence of damage events occurred at the internal edge. First, the internal edge fails. This is evidenced by the region between the internal and free edges being intact and separated from the rest of the laminate after ultimate failure.

After failure of the internal discontinuity, the likelihood of delamination emanating from the internal edge increases. Again the $+15/-15$ interface is delamination critical and grows internally. However, the region between the internal and free edges does not delaminate, because the interlaminar stresses

Table 2 Predicted and experimental delamination initiation and ultimate strains

Laminate	Prediction: Resin pocket, μstrain	Prediction: Ply analogy, μstrain	Experimental: Initiation, μstrain (C.V. %)	Experimental: Initial failure mode	Experimental: Ultimate, μstrain (C.V. %)
$[0/\pm 15]_s$	NA	NA	6420 (11.8)	Free-edge delamination	8643 (5.8)
$[0/+15/-15]_s$	NA	6381	6547.5 (11.0)	Internal edge	8447.5 (3.9)
$[0/+15/-30/-15]_s$	6015	7380	5905.0 (5.5)	Internal edge & free-edge delamination	9297.5 (4.5)
$[0/+15/-15/]_s$	NA	4998	5850.0 (8.3)	Internal edge & free-edge delamination	8395.0 (2.5)
$[0/+15/-15/+45]_s$	4062	6306	5834.4 (13.5)	Internal edge	8943.8 (9.2)
$[\pm 15/0]_s$	NA	NA	5398 (8.7)	Free-edge delamination	7535 (5.4)
$[+15/-15/0]_s$	NA	5751	5712.5 (26.9)	Internal edge	9460.0 (6.2)
$[+15/-15/+30/0]_s$	6005	7392	5377.5 (11.6)	Internal edge	8682.5 (3.4)
$[+15/-15/0/]_s$	NA	10,782	5957.5 (4.0)	Free-edge delamination	6247.5 (15.6)
$[+15/-15/0/+15]_s$	7673	11,998	6247.5 (4.1)	Free-edge delamination & internal edge	7487.5 (3.4)

in it are not as critical as indicated in Fig. 4 by the two lines designated as $[0/+15/-30/-15]_s$ failed internal edge and $[0/+15/-30/-15]_s$ free edge. As the delamination grows toward the centerline of the specimen, unlike the free-edge problem, the delaminated region is constrained in the transverse direction. Accordingly, the ultimate strain is increased, as evidenced in Table 2.

Often, more than one significant damage event was recorded via the strain gage and load cell data. Because each specimen was examined after ultimate failure, the initial point of failure could be deduced. If the internal edge failed, then damage would be located at the internal edge and inward toward the longitudinal centerline of the specimen. Here the region between the internal and free edges would be intact. If free-edge delamination occurred, the damage would be clearly observable. Here the damage would extend over the entire width of the specimen. The initial failure for each specimen type is given in Table 2. If more than one failure type is given, the one that occurred a majority of the time is listed first.

Strength Predictions

The strength of the internal edge is determined from the results of the finite element analysis. For material discontinuities, the in-plane state of stress across the discontinuity or the state of stress in the resin pocket is used. For longitudinal ply drops, the stresses in the resin pocket are used. The strengths of the basic unidirectional ply and the neat resin used in this study are given in Table 1.

In-Plane

The in-plane stress state at the discontinuity is determined by averaging the stress state in the elements on either side of the discontinuity. The calculated stress state at the internal discontinuity is placed into the Tsai-Wu failure criterion.[9] In tensor form this criterion is:

$$F_{1111}\sigma_{11}^2 + 2F_{1122}\sigma_{11}\sigma_{22} + F_{2222}\sigma_{22}^2 + 4F_{1212}\sigma_{12}^2 + F_{11}\sigma_{11} + F_{22}\sigma_{22} = 1 \quad (1)$$

where $F_{\alpha\beta\sigma\gamma}$ and $F_{\alpha\beta}$ are constants determined from the characteristic strengths of the unidirectional ply. The interaction term F_{1122} is found by the following equation:

$$F_{1122} = -\tfrac{1}{2}\sqrt{F_{1111}F_{2222}} \quad (2)$$

Because the finite element model is linear, the actual failure strain can be scaled from the applied test case.

This analysis is performed on the four laminates in this study involving a material discontinuity. The stresses across the discontinuity in the axis system, defined by the orientation of the discontinuity (i.e., the loading axes in this study), are used in the criterion. These predictions are provided in Table 2 for the laminates tested experimentally. To illustrate the effect of the angle at which the material is reoriented, this prediction is shown in Fig. 8 for the basic laminate designated as $[0/+15|\sigma/-15]_s$ vs α.

Resin Pocket

The second strength prediction is based on the strength of the resin pocket at the discontinuity. In the longitudinal ply drop specimens, the size of the resin pocket is significant at the terminated ply. In the specimens with a material discontinuity, the width of the resin pocket is assumed to be 0.5-ply thicknesses (0.067 mm).

To determine if the calculated stress state within a given resin element is critical or not, the von Mises stress is determined:

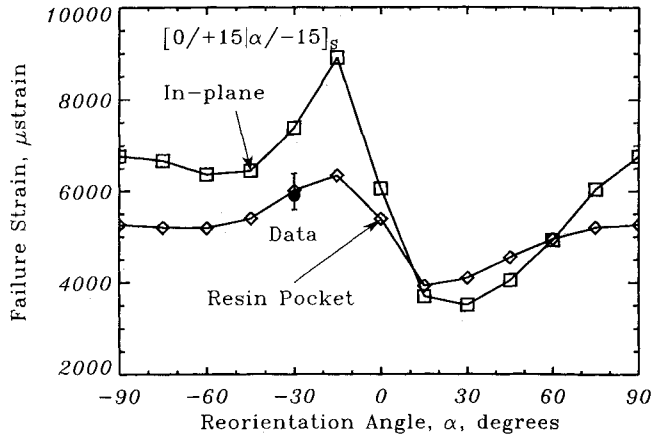

Fig. 8 Experimental data and strength predictions for damage initiation of $[0/+15|\alpha/-15]_s$ laminates.

$$\sigma = \{\tfrac{1}{2}[(\sigma_{22}-\sigma_{33})^2 + (\sigma_{33}-\sigma_{11})^2 + (\sigma_{11}-\sigma_{22})^2] + 3\sigma_{23}^2 + 3\sigma_{31}^2 + 3\sigma_{12}^2\}^{1/2} \quad (3)$$

If the von Mises stress is equal to the characteristic strength of the resin σ_0, failure is assumed to occur. Any effects that the fibers may have on this strength are neglected in the current study. This analysis is conducted on all of the specimens considered in this study, both the laminates with a parallel ply drop and the laminates with a material discontinuity, and the results are presented in Table 2 for the laminates tested experimentally. Again, to illustrate the effect of the angle which the material is reoriented, this prediction is shown in Fig. 8 for the basic laminate designated as $[0/+15|\alpha/-15]_s$ vs α.

Discussion

Table 2 indicates the ability of the two models to predict the strength of an internal discontinuity. In general, the criterion based on the in-plane stress state averaged at the internal edge predicts a greater strength, as shown in Fig. 8. In one of the laminate types, $[+15/-15/0|+15]_s$ both strength criteria predict relatively higher strains compared to the other laminates. In particular, these strains are well above the level at which free-edge delamination occurs in the laminate tested. In this case, the specimen will fail as a result of free-edge delamination, rather than as a result of the failure of the internal edge. This is supported by the postmortem analysis.

An excellent correlation is seen for the laminates with an angle discontinuity in the second and fifth plies $[0/+15|-30/-15]_s$ and $[+15/-15|+30/0]_s$. Here the resin pocket model predicts failure that is within the scatter of the data. Because the model does not take into account any flaws that may exist as a result of the manufacturing process, experimental values should be lower than predicted values. This is indicated by the results.

For the $[0/+15/-15|+45]_s$ laminates, the experimental data fall between the two criteria. For this laminate, the resin model predicts a strain level of 4062 microstrain. If damage had initiated at this level, it may have resulted in a load drop well in the noise level of the experiment. Thus, the initial damage event may have gone undetected.

In the last laminate $[+15/-15/0|-15]_s$, failure was dominated by free-edge delamination and the internal edge is not critical. This correlates with the relatively high predictions of the two criteria. Thus, the models accurately predict that the interface is not critical.

In terms of the longitudinal ply drops, the resin pocket model predicts the initiation of damage very well. In the three laminates dominated by internal edge failures, the model predicts failure within the scatter of the data. In the one laminate dominated by free-edge delamination, the model predicts a

strain level almost twice the observed level. Again the model does well to indicate a noncritical discontinuity. Thus, as in any failure prediction, all other failure mechanisms must be accounted to be able to predict the overall response.

Conclusions

A methodology has been formulated to determine the strength of longitudinal discontinuities in laminated composites. The methodology proposed is independent of the analytical method used to determine the stress state and the specific failure criteria employed. Any acceptable method to determine the stress state at and around the discontinuity can be used in combination with any isotropic failure criterion or any single-ply failure criterion. The specific analytical tools and failure criteria employed herein merely illustrate the validity of the resin pocket model. Moreover, in the unidirectional ply analogy, a simplistic approach predicts the onset of damage well. The methodology presented serves as the framework for further work.

From the analytical work performed in this study and the corresponding experimental evidence, the following conclusions are made:

1) The use of the stress state of plies in an unidirectional analogy provides an approximate prediction of the strength of longitudinal discontinuities. However, such predicted values in this study typically were higher than the observed strength.

2) Modeling a discontinuity with an associated resin pocket provides direct evaluation of the stresses in the region where failure occurs. A good correlation is observed when the stress state in this matrix pocket is used in an isotropic failure criterion.

3) Longitudinal ply drops and discontinuous angle alterations create a potentially weak interface in the laminate. Thus, failure of longitudinal discontinuities may severely limit the performance of laminated composites by providing additional sites for delamination initiation.

Acknowledgments

This work was supported by the Army Research Office under Contract DAAG-29-83K0002. Thomas Doligalshi was the contract monitor. The author thanks William R. Pogue, III, who performed the experimental portion of this work.

References

[1]Kemp, B. L., and Johnson, E. R., "Response and Failure Analysis of a Graphite/Epoxy Laminate Containing Terminating Internal Plies," *Proceedings of the AIAA/American Society of Mechanical Engineers/American Society of Civil Engineers/American Helicopter Society Twenty-sixth Structures, Structural Dynamics and Materials Conference,* Orlando, FL, April 15–17 1985, pp. 13–24.

[2]Curry, J. M., Johnson, E. R., and Starnes, J. H., Jr., "Effect of Dropped Plies on the Strength of Graphite-Epoxy Laminates," *Proceedings of the AIAA/American Society of Mechanical Engineers/American Society of Civil Engineers/American Helicopter Society Twenty-ninth Structures, Structural Dynamics and Materials Conference,* Monterey, CA, April 6–8, 1987, pp. 737–747.

[3]Fish, J. C., and Lee, S. W., "Edge Effects in Tapered Composite Structures," *National Technical Specialists' Meeting on Advanced Rotorcraft Structures,* Hampton, VA, Oct. 1988.

[4]Vizzini, A. J., "Prevention of Free-Edge Delamination via Edge Alteration," *Proceedings of the AIAA/American Society of Mechanical Engineers/American Society of Civil Engineers/American Helicopter Society Twenty-ninth Structures, Structural Dynamics and Materials Conference,* Williamsburg, VA, April 1988, pp. 365–370.

[5]Pogue, W. R., III, and Vizzini, A. J., "Structural Tailoring Techniques to Prevent Delamination in Composite Laminates," *American Helicopter Society,* Vol. 35, No. 4, Oct. 1990, pp. 38–45.

[6]Lee, S. W., Rhiu, J. J., and Wong, S. C., "Hybrid Finite Element Analysis of Free Edge Effect in Symmetric Composite Laminates," TR, Department of Aerospace Engineering, University of Maryland, College Park, MD, June, 1983.

[7]Fish, J. C., and Lee, S. W., "Strength of Glass-Epoxy Laminates Based on Interply Resin Failure," *Proceedings of the American Society of Composites Third Technical Conference,* Seattle, WA, Sept. 1988, pp. 242–252.

[8]Brewer, J. C., and Lagace, P. A., "Quadratic Stress Criterion for Initiation of Delamination," *Journal of Composite Materials,* Vol. 22, No. 12, 1988, pp. 1141–1155.

[9]Tsai, S. W., and Wu, E. M., "A Generalized Theory of Strength for Anisotropic Materials," *Journal of Composite Materials,* Vol. 5, 1971, pp. 55–80.